

## Electrochemical Investigation of Phenol Oxidation by a TiO<sub>2</sub>/GAC Based Packed-Bed Electrode Reactor

Qing Chen<sup>1</sup>, Lizhang Wang<sup>1,\*</sup>, Yuehua Xu<sup>1</sup>, Peng Li<sup>2</sup>, Xiao Wang<sup>1</sup>, Mingze Wang<sup>1</sup>, Ying Kong<sup>1</sup>

<sup>1</sup> School of Environment Science and Spatial Informatics, China University of Mining and Technology, Xuzhou City, Jiangsu 221116, PR China;

<sup>2</sup> School of Water Resource & Environmental Engineering, East China Institute of Technology, Nanchang, Jiangxi 330013, PR China

\*E-mail: [wlzh0731@126.com](mailto:wlzh0731@126.com)

Received: 2 April 2018 / Accepted: 1 June 2018 / Published: 5 July 2018

---

In this work, TiO<sub>2</sub>/GAC was prepared by sol-gel method and employed as particulate electrode for efficient phenol oxidation. The X-ray Diffraction (XRD) and X-ray photoelectron spectroscopy (XPS) analysis reveal the titanium dioxide loaded on GAC exists in anatase TiO<sub>2</sub> state. Compared to the GAC electrode, the TiO<sub>2</sub>/GAC can enhance feedback current and catalytic-oxidation ability, which could be obtained through cyclic voltammetry (CV) and electrochemical impedance spectroscopy (EIS) measurements. Furthermore, the excellent electrochemical performance of TiO<sub>2</sub>/GAC is validated by the increase of phenol and chemical oxygen demand (COD) removal and obvious decrease of the power consumption during bulk electrolysis of phenolic wastewater.

---

**Keywords:** phenol; TiO<sub>2</sub>/GAC; packed-bed electrode reactor; catalytic-oxidation performance

### 1. INTRODUCTION

During the past several decades, electrochemical processes with unique features of simplicity, robustness and high operation efficiency have been introduced into treating wastewater containing different organic pollutants [1-3]. The dimensionally stable anodes (DSAs) are usually employed due to their strong ability in producing reactive hydroxyl radicals ( $\cdot\text{OH}$ ) which are responsible for effective electro-oxidation. To further improve the electrode performances, a three dimension structure equipped with granular activated carbon (GAC) is developed to expand electrode area via GAC bipolarity in the electric field [4-6]. However, this kind of framework is still restricted by excessive oxygen evolution of carbon material and cost-efficient goal toward electro-oxidation is difficult to be achieved through this way. As known that usage of the metal oxide e.g. SnO<sub>2</sub> [7, 8] and PbO<sub>2</sub> [9, 10] could effectively

increase the oxygen evolution potential (OEP) of anodes, maybe employment of such oxides supported GAC particles also would be a feasible approach for enhancing current efficiency and decreasing power cost during organic wastewater treatment.

In this work, GAC loaded  $\text{TiO}_2$  ( $\text{TiO}_2/\text{GAC}$ ) was prepared by sol-gel method and employed as particulate electrode for phenol degradation. The phase composition of the  $\text{TiO}_2/\text{GAC}$  was detected by X-ray diffraction (XRD) and X-ray photoelectron spectroscopy (XPS) techniques. Electrochemical tests i.e. cyclic voltammetry (CV) and electrochemical impedance spectroscopy (EIS) conducted on an electrochemical workstation by using three-electrode system were carried out to investigate electrode performances of the prepared  $\text{TiO}_2/\text{GAC}$ . In addition, GAC together with  $\text{TiO}_2/\text{GAC}$  based packed-bed reactor for phenolic wastewater treatment were performed to verify the oxidation enhancement of the  $\text{TiO}_2/\text{GAC}$  particulate electrode via chemical oxygen demand (COD) removal efficiency, current yield and power consumption.

## 2. EXPERIMENTAL

### 2.1. Chemicals and materials

Phenol (Merck, in 99.5% pure) and sodium sulfate ( $\text{Na}_2\text{SO}_4$ ) in analytical pure were used to prepare the raw solution. Others reagents such as ethanol, hydrochloric acid, acetic acid and tetrabutyl titanate were also obtained in analytical pure.

$\text{PbO}_2/\text{Ti}$  anodes with  $2 \times 2$  cm and  $10 \times 10$  cm dimension, which were used for electrochemical tests and phenol oxidation, respectively, were provided by Qixin Company (China). GAC particles having an average particle size of 5 mm, a specific weight of  $752 \text{ g L}^{-1}$  and a specific surface area of  $826 \text{ m}^2 \text{ g}^{-1}$  according to BET method were employed for construction of a GAC based packed-bed electrode reactor and preparation of  $\text{TiO}_2/\text{GAC}$  particulate electrode.

### 2.2. $\text{TiO}_2/\text{GAC}$ preparation and performances characterization

Prior to experiments, GAC particles were washed several times by deionized water to remove the fines and ashes and dried in an oven at  $105 \text{ }^\circ\text{C}$  for 24 h to a constant weight. The  $\text{TiO}_2/\text{GAC}$  was achieved by the sol-gel method which contained three steps: (1) preparation of the precursor reagents including solutions A (35 mL ethanol, 32 mL distilled water and 0.6 mL hydrochloric acid) and B (70 mL ethanol, 23 mL acetic acid and 35 mL tetrabutyl titanate); (2) aged stage: pour A to B using a separating funnel at speed of  $4 \text{ mL min}^{-1}$  with stirring ( $500 \text{ r min}^{-1}$ ) and put the GAC particles into the mixture solution and try to make them well-distributed and then it should be aged for 2 days; (3) baked process: the prepared solution with GAC was moved into an oven to be dried at  $105 \text{ }^\circ\text{C}$  under nitrogen protection for 7 h, and then baked according to the following procedure: increase the temperature from  $0 \text{ }^\circ\text{C}$  to  $200 \text{ }^\circ\text{C}$  in 30mins and maintain  $200 \text{ }^\circ\text{C}$  for 1 h, raise temperature from  $200 \text{ }^\circ\text{C}$  to  $500 \text{ }^\circ\text{C}$  in 40 mins and then maintain  $500 \text{ }^\circ\text{C}$  for another 2 h.

XRD patterns were obtained on a XRD diffractometer (type: D8 Advance Bruker Corp) with  $\text{CuK}\alpha$  radiation at tube voltage/current 40 kV/30 mA, and  $\lambda$  of 1.5406 Å. XPS (ESCALAB 250Xi, ThermoFisher Corp) was conducted with  $\text{AlK}\alpha$  X-ray source of energy 1253.6 eV at a power of 240 W. The pressure in the analysis chamber was maintained below  $2 \times 10^{-9}$  mbar during the measurements.

The performances of GAC and  $\text{TiO}_2/\text{GAC}$  particulate electrodes were carried out on an electrochemical workstation (Zahner Corp, IM6) with 0.25 M  $\text{Na}_2\text{SO}_4$  and 0.01 M phenol solution by a three-electrodes system composed of  $\text{PbO}_2/\text{Ti}$  anode (2×2 cm), Pt counter electrode (4×4 cm) and saturated calomel electrode (SCE) as a reference electrode at temperature of 25 °C. The scanning rate for CV test was 50 mV s<sup>-1</sup> and the EIS cures were obtained at open circuit potential of 0.53 V.

### 2.3. Electrochemical reactor and phenol bulk oxidation

The electrochemical process for bulk electrolysis was composed of eight cells constructed by polymethyl methacrylate plastics and a D.C power modeled KXN-1540D. Each cell was equipped with  $\text{PbO}_2/\text{Ti}$  and Ti electrodes (10 cm×10 cm) with inter-electrode distance of 5 cm and a peristaltic pump. The cells were packed with GAC or  $\text{TiO}_2/\text{GAC}$  and the detailed information for the cell and process were provided elsewhere [11]. Synthetic phenolic wastewater (0.01 M phenol and 0.25 M  $\text{Na}_2\text{SO}_4$ ) was oxidized at flow rate of 0.6 L h<sup>-1</sup> and current density of 100 A m<sup>-2</sup> under continuous mode.

### 2.4. Analytical methods

A Spectrophotometer UV-visible (UV-1800, Shimadu) was used to detect phenol concentration and COD of each sample was determined by the standard method [12]. The average current efficiency (ACE, %) and power consumption ( $E_{\text{sp}}$ , kWh kg<sup>-1</sup> COD) were calculated according to the following equations, respectively [13].

$$\text{ACE} = F \xi V \frac{(\text{COD}_0 - \text{COD}_t)}{8It} \times 100\%$$

(1)

$$E_{\text{sp}} = \frac{3600UI}{q(\text{COD}_0 - \text{COD}_t)}$$

(2)

where  $F$  is Faraday constant (96,485 C mol<sup>-1</sup>),  $\xi$  the porosity of the packed-bed electrode cell (here its value is about 0.42),  $V$  the volume of each cell (L),  $t$  the residence time (s),  $I$  the current (A),  $U$  the applied voltage (V),  $q$  the flow rate (L h<sup>-1</sup>),  $\text{COD}_0$  and  $\text{COD}_t$  (g L<sup>-1</sup>) the initial COD and COD at time  $t$ , respectively.

## 3. RESULTS AND DISCUSSION

### 3.1. Surface composition of $\text{TiO}_2/\text{GAC}$

Fig. 1 shows the XRD patterns of the  $\text{TiO}_2/\text{GAC}$  and GAC particles. From this figure, strong diffraction peaks at angles of 25.363°, 37.008°, 37.862°, 38.625°, 48.095°, 53.944°, 55.110°, 62.166°,

62.743°, 68.814°, 70.345°, 75.103° and 76.090° are observed, which are indexed to anatase TiO<sub>2</sub> phase according to JCPDS no. 65-5714; while the diffraction peaks of GAC are located at angles of 21.004°, 22.890°, 26.522°, 36.026°, 43.310°, 50.493° and 60.153° (JCPDS no. 50-0927). In addition, the regular distribution of these peaks illustrates the TiO<sub>2</sub> crystal is even loaded at the surface or into the mesopore/micropore of GAC particles, which could be interpreted by crystallite parameter calculated from the peaks and half-height of lattice planes (101), (103), (004), (112), (200), (105), (211), (204), (116) and (220) using the Scherrer equation [14]; these results are given in Table 1.

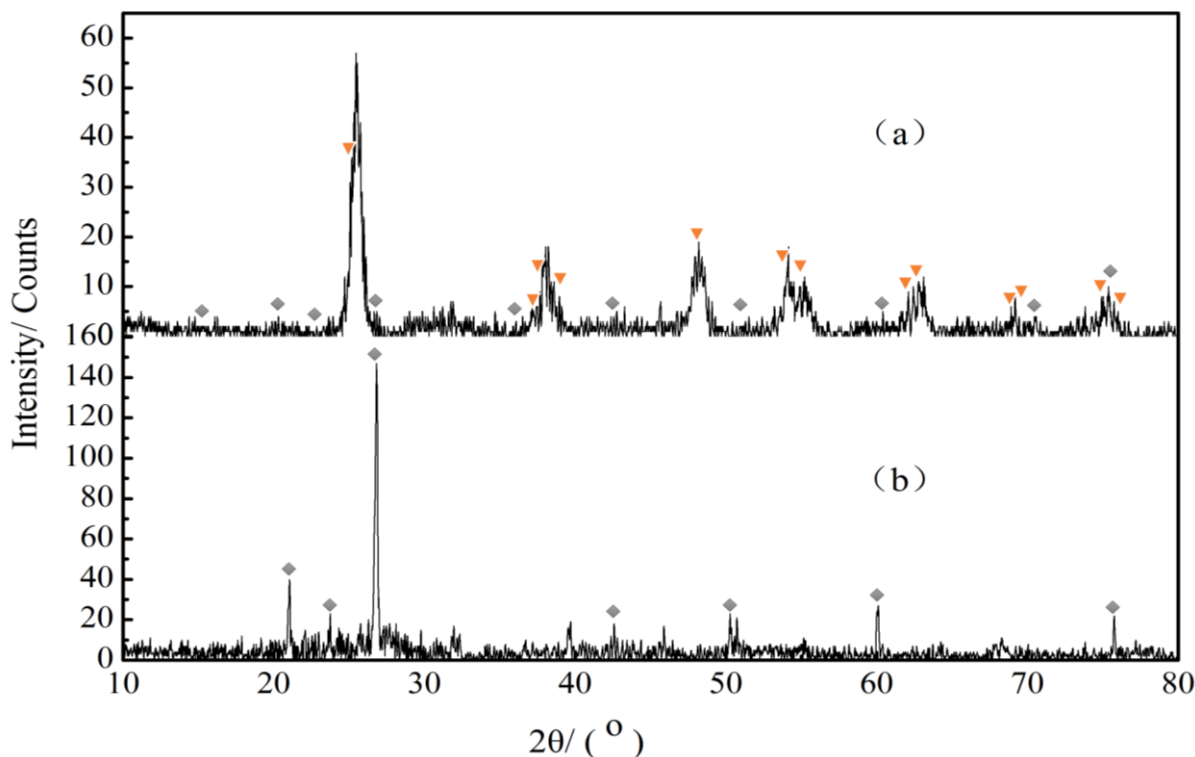


**Figure 1.** XRD patterns of TiO<sub>2</sub>/GAC (a) and GAC (b). Phases: ◆, C; ▼, TiO<sub>2</sub>

**Table 1.** Theoretical and experimental crystallite parameters of the prepared TiO<sub>2</sub>/GAC

Lattice planes ( <i>hkl</i> )	101	103	004	112	200	105	211	204	116	220
Theoretical [15]	0.3510	0.2424	0.2379	0.2334	0.1890	0.1699	0.1664	0.1480	0.1362	0.1339
Experimental	0.3513	0.2315	0.2376	0.2321	0.1820	0.1532	0.1664	0.1482	0.1269	0.1324

The XPS survey spectra in Fig. 2a provide the existence of atomic species on surface of the prepared TiO<sub>2</sub>/GAC, which are oxygen, titanium, carbon and chlorine (detection of aluminum is due to system error) and their atomic ratios are 55.83%, 21.76%, 10.18% and 7.03%, respectively. High

accuracy spectrum of Ti2p (Fig. 2b) for Ti2p<sub>3/2</sub> together with Ti2p<sub>1/2</sub> at binding energies of 458.8 eV and 465.04 eV indicates there is only one Ti atom in TiO<sub>2</sub>, and the difference of binding energy for the two states is 6.24 eV, which is slightly higher than that of other work [16]; this may be caused by error of different instruments. The spectrum of O1s in Fig. 2c validates that most of oxygen atom is bonded with Ti at binding energy of 533.0 eV and 530.8 eV. Hence, these results confirm that titanium dioxide is successfully loaded on the surface of GAC particles.

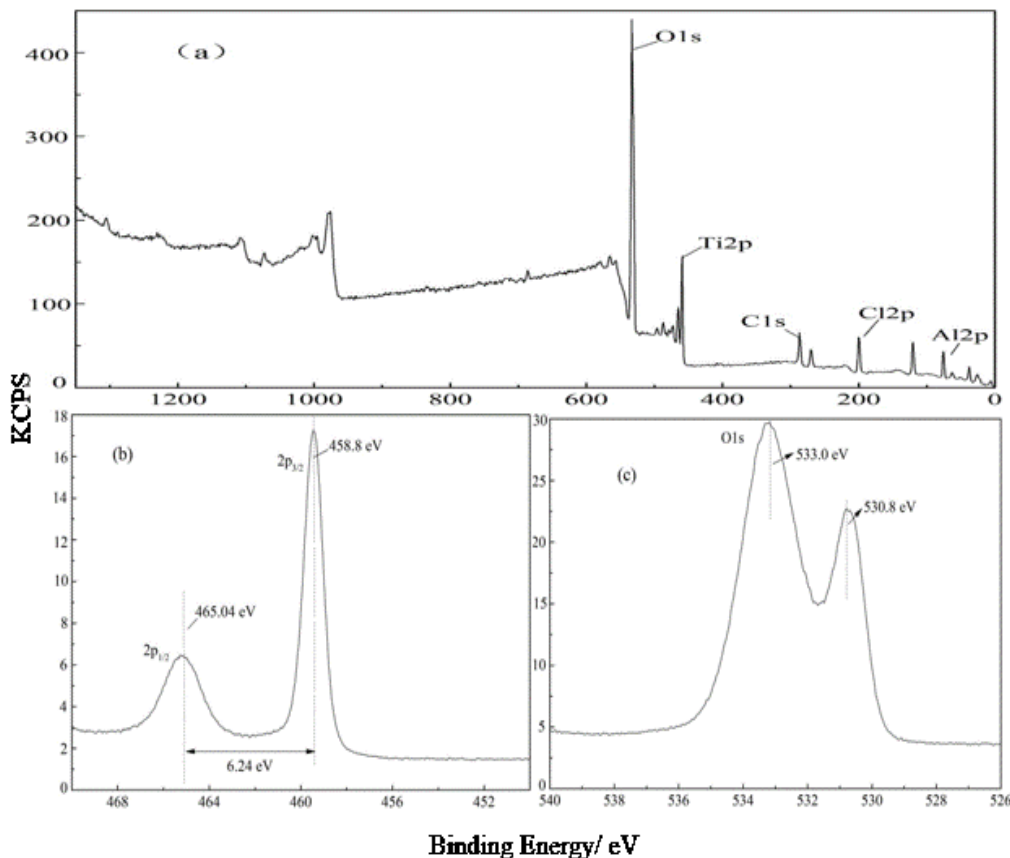


**Figure 2.** XPS spectra for TiO<sub>2</sub>/GAC particulate electrode (a), Ti 2p (b) and O1s (c) peaks

### 3.2. Electrode performances

Fig. 3 depicts the CV curves of GAC and TiO<sub>2</sub>/GAC coupled with PbO<sub>2</sub>/Ti anode conducted in hybrid of 0.25 M Na<sub>2</sub>SO<sub>4</sub> and 0.01 M phenol within potential window from 0 to 2.5V (vs. SCE) at 50 mV s<sup>-1</sup>. The two asymmetrical curves without redox peaks indicate the reactions in the system should be irreversible and phenol could be directly oxidized at surface of the anode and particulate electrodes [17-19]. In addition, compared with GAC, larger feedback current is shown when the TiO<sub>2</sub>/GAC is employed, which illustrates the oxidative ability of the particulate electrode could be enhanced by loading TiO<sub>2</sub>. Voltammetric charge (*Q*) is usually used to evaluate active spot of anodes and it could be calculated according to CV curve by the following equation:

$$Q = \frac{\int_{U_1}^{U_2} i dv}{U_2 - U_1} \quad (3)$$

where  $U_1$  and  $U_2$  are the initial and final potential (V),  $i$  the feedback current (A) and  $v$  the scanning rate ( $\text{mV s}^{-1}$ ). By using Eq. (3), the parameter  $Q$  of the GAC and  $\text{TiO}_2/\text{GAC}$  are obtained with values of 0.23 C and 0.38 C, respectively; in this sense, the prepared  $\text{TiO}_2/\text{GAC}$  electrode should possess abilities of enhancing phenol removal efficiency and current yield during bulk electrolysis.

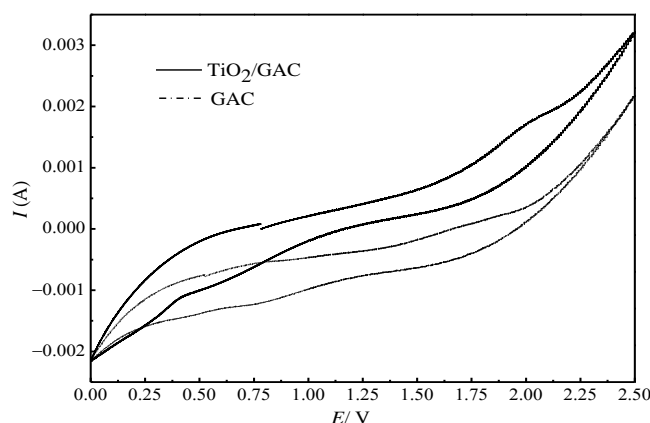


**Figure 3.** CV curves of GAC and  $\text{TiO}_2/\text{GAC}$  coupled with  $\text{PbO}_2/\text{Ti}$  anode in solution containing 0.25 M  $\text{Na}_2\text{SO}_4$  and 0.01 M phenol at scanning rate of  $50 \text{ mV s}^{-1}$

The Nyquist complex plane impedance spectra of GAC and  $\text{TiO}_2/\text{GAC}$  are presented in Fig. 4. A relatively lower semicircle diameter at high frequency is observed if the  $\text{TiO}_2/\text{GAC}$  is used, which indicates the resistance for charge transfer could be effectively decreased by loading  $\text{TiO}_2$  catalyst. The inclined lines approximating to  $45^\circ$  angle demonstrate that better electron-diffusion process is achieved on carbon electrodes regardless of the existence of the  $\text{TiO}_2$  [14, 20, 21]. The equivalent electric circuit is provided in Fig. 4b, within which  $R_e$  is the electrolyte resistance;  $C_1$ ,  $C_2$  and  $R_1$ ,  $R_2$  the capacitance and resistance of the surface film formed on anode and carbon electrodes, respectively;  $C_{fp}$  and  $C_p$  the capacitance formed due to gradually voltage decrease;  $R_{ct}$  the charge-transfer resistance and  $Z_w$  the Warburg impedance related to the diffusion of electrons into the carbon electrodes. The exchange current density  $i_0$  can be calculated by parameter  $R_{ct}$  as follows [22]:

$$i_0 = RT / nFR_{ct} \quad (4)$$

where  $R$  is the gas constant ( $8.314 \text{ J mol}^{-1} \text{ K}^{-1}$ ),  $T$  the absolute temperature (K) and  $n$  the number of transferred electrons during phenol oxidation (here  $n=4$ ).

The simulated results and calculated  $i_0$  values of the two particulate electrodes are summarized in Table 2. It can be seen that the values of  $R_e$  and  $R_1$  are almost equal when GAC and  $\text{TiO}_2/\text{GAC}$  are used, while the values of  $R_2$  and  $R_{ct}$  for the two particulate electrode are quite different. In the presence of the  $\text{TiO}_2$  catalyst, the  $R_2$  value decreases to  $6.84 \Omega$ , which is only about one fourth of that for GAC based packed-bed electrode reactor, indicating the electron transfer rate for phenol oxidation would be effectively accelerated. In addition, compared with GAC,  $R_{ct}$  values obviously decreases from  $329.3 \Omega$  to  $206.5 \Omega$ , resulting into the increase of  $i_0$  values from  $1.83 \times 10^{-6} \text{ A cm}^{-2}$  to  $2.92 \times 10^{-6} \text{ A cm}^{-2}$ . Both the

$R_2$  decrease and  $i_0$  increase are beneficial to efficient phenol degradation, which directly confirm the employment of  $\text{TiO}_2/\text{GAC}$  as particulate electrode is a better alternative compared with GAC particles.

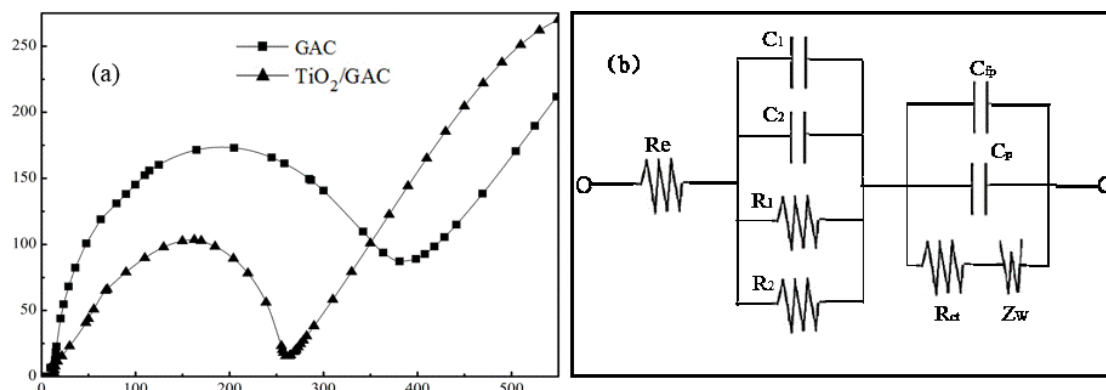


**Figure 4.** The EIS (a) and equivalent electric circuit (b) of GAC and  $\text{TiO}_2/\text{GAC}$  coupled with  $\text{PbO}_2/\text{Ti}$  anode in solution containing 0.25 M  $\text{Na}_2\text{SO}_4$  and 0.01 M phenol at the open circuit potential of 0.53 V

**Table 2.** Summary of the EIS simulated results and  $i_0$  values of the GAC and  $\text{TiO}_2/\text{GAC}$  electrodes

Electrodes	$R_e$ ( $\Omega$ )	$R_1$ ( $\Omega$ )	$R_2$ ( $\Omega$ )	$R_{ct}$ ( $\Omega$ )	$i_0 \times 10^{-6}$ ( $\text{A cm}^{-2}$ )
GAC	5.88	0.33	29.33	329.3	1.83
$\text{TiO}_2/\text{GAC}$	4.63	0.35	6.84	206.5	2.92

### 3.3. Bulk electrolysis

The comparison of the two particulate electrodes for phenol oxidation is shown in Fig. 5. It can be seen from Fig. 5a that both COD and phenol removal efficiency are significantly enhanced if the prepared  $\text{TiO}_2/\text{GAC}$  is used, leading to obvious increase of current yield and decrease of specific power consumption (Fig. 5b). After 224 minutes treatment, the effluent concentrations of COD and phenol by using  $\text{TiO}_2/\text{GAC}$  are  $123.6 \text{ mg L}^{-1}$  and  $7.1 \text{ mg L}^{-1}$ , respectively, which are increased by ratios of 77.3% and 96.2% compared with those of GAC particles ( $544.2 \text{ mg L}^{-1}$  and  $185.6 \text{ mg L}^{-1}$ , respectively). Such enhancement is mainly for electrode area expansion and decrease of the oxidation resistance evoked by  $\text{TiO}_2$  catalytic performance [23], further validating the excellent oxidation ability of  $\text{TiO}_2/\text{GAC}$  for degradation of organic pollutants.

From the engineering purpose, it is also of great concern the superiority of the  $\text{TiO}_2/\text{GAC}$  based packed-bed electrode reactor in cost-effective property. The experimental results conducted at current density of  $100 \text{ A m}^{-2}$  and flow rate of  $0.6 \text{ L h}^{-1}$  show the average current efficiencies of  $\text{TiO}_2/\text{GAC}$  are always higher than those without  $\text{TiO}_2$  catalyst together with the decrease of the power consumption at the same reaction time (Fig. 5b). When the reaction time is 224 min, the current yield increases from 30.6% to 38.5% and the power consumptions decrease from  $159.6 \text{ kWh kg}^{-1}$  COD to  $126.8 \text{ kWh kg}^{-1}$  COD in the absence and presence of  $\text{TiO}_2$  catalyst. It is worth noting that the power cost is obviously

lower than the three works conducted by using  $\gamma$ - $\text{Al}_2\text{O}_3$  particulate electrode for chloramphenicol (CAP) oxidation ( $222.7 \text{ kWh kg}^{-1}$  CAP) [24] and modified kaolin particulate electrode for anionic surfactants degradation at (about  $816 \text{ kWh kg}^{-1}$  COD with COD removal efficiency of 76%) [25]. Therefore, the increase of oxidation rate and decrease of power consumption by the  $\text{TiO}_2/\text{GAC}$  particulate electrode could simultaneously reduce the reactor volume and running cost, making the technology more attractive from an economic point of view.

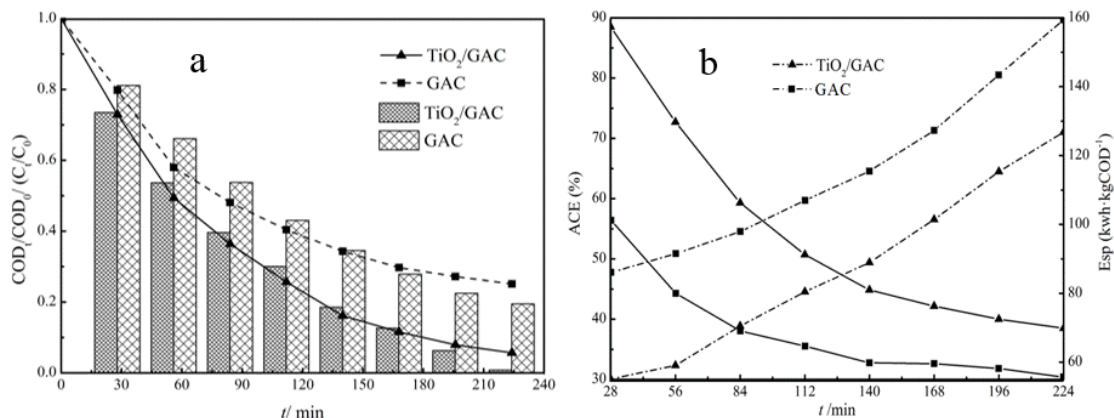


**Figure 5.** Dependence of COD and phenol concentration (a), ACE and  $E_{sp}$  (b) on reaction time during phenolic wastewater treatment at current density of  $100 \text{ A m}^{-2}$  and flow rate of  $0.6 \text{ L h}^{-1}$ . Notes: (a) the lines and bars depict the COD and phenol concentration, and (b) ACE and  $E_{sp}$  are described by solid and dotted lines, respectively.

#### 4. CONCLUSION

The employment of GAC and  $\text{TiO}_2/\text{GAC}$  prepared by sol-gel method as particulate electrodes coupled with  $\text{PbO}_2/\text{Ti}$  anode was investigated for phenol oxidation in this work. The XRD and XPS results reveal that the anatase  $\text{TiO}_2$  exists at surface or in mesopore/micropore of GAC particles. Compared to GAC particles, the voltammetric charge of the prepared  $\text{TiO}_2/\text{GAC}$  is increased from  $0.23 \text{ C}$  to  $0.38 \text{ C}$  and oxidation resistance is obviously decreased from  $329.3 \Omega$  to  $206.5 \Omega$ , leading to the increase of exchange current density from  $1.83 \times 10^{-6} \text{ A cm}^{-2}$  to  $2.92 \times 10^{-6} \text{ A cm}^{-2}$  during phenol degradation; moreover, the bulk electrolysis show that the effluent COD and power consumption low to values of  $185.6 \text{ mg L}^{-1}$  and  $126.8 \text{ kWh kg}^{-1}$  COD under conditions of flow rate  $0.6 \text{ L h}^{-1}$ , current density  $100 \text{ A m}^{-2}$  and reaction time 224 minutes, which are decreased by ratios of 77.3% and 20.6% to those of GAC particulate electrode, respectively, directly validating the higher catalytic-oxidation ability of the prepared  $\text{TiO}_2/\text{GAC}$  particulate electrode in degradation of organic pollutants.

#### ACKNOWLEDGEMENTS

The authors thank for the financial support by the Key Research & Development Plan of Jiangsu Province (BE2017640) and the Xuzhou Science and Technology Plan Project (KC16SS090). Mr. Q. Chen acknowledges the financial support by the Postgraduate Research & Practical Innovation Program of Jiangsu Province (SJCX17\_0523).

## References

1. X.Z. Zhou, S.Q. Liu, A.L. Xu, K.J. Wei, W.Q. Han, J.S. Li, X.Y. Sun, J.Y. Shen, X.D. Liu, L.J. Wang, *Chem. Eng. J.*, 330 (2017) 956.
2. R.M. Farinos, A.M. Ruotolo Luís, *Electrochim. Acta*, 224 (2017) 32.
3. Y.H. Zhang, K.J. Wei, W.Q. Han, X.Y. Sun, J.S. Li, J.Y. Shen, L.J. Wang, *Electrochim. Acta*, 189 (2016) 1.
4. Y. Feng, X. Li, T. Song, L.S. Fan, Y.Z. Yu, J.Y. Qi, X.W. Wang, *Ecol. Eng.*, 101 (2017) 21.
5. B. Shen, X.H. Wen, X. Huang, *Chem. Eng. J.*, 327 (2017) 597.
6. K.W. Jung, M.J. Hwang, D.S. Park, K.H. Ahn, *Sep. Purif. Technol.*, 146 (2015) 154.
7. N.D. Zhang, N. Li, Y.Z. Peng, *Acta Phys-Chim. Sin.*, 19 (2003) 1154.
8. F. Stéphane, N. Tina, B. Helmut, Ch. Comninellis, *Electrochem. Commun.*, 9 (2007) 1969.
9. M. Errami, R. Salghi, N. Abidi, L. Bazzi, B. Hammouti, A. Chakir, E. Roth, S.S. Al-Deyab, *Int. J. Electrochem. Sci.*, 6 (2011) 4927.
10. Ch. Comninellis, C. Pulgarin, *J. Appl. Electrochem.*, 23 (1993) 108.
11. L.Z. Wang, Y.L. Hu, Y.L. Zhang, P. Li, Y.M. Zhao, *Sep. Purif. Technol.*, 109 (2013) 18.
12. APHA. Standard methods for examination of water and wastewater, 20th ed. Washington DC: APHA; 1998.
13. L.Z. Wang, Y. Kong, D. Wei, Y. Kong, P. Li, X. Jiao, *Int. J. Electrochem. Sci.*, 12 (2017) 8120.
14. F. Kenji, K. Kazuhiko, I. Kennichi, Y. Masaki, *J. Power sources*, 69 (1997) 165.
15. N. Yang, W. Yue, The handbook of inorganic matelloid materials atlas, Wuhan Ind. Univ. Press, (2000) Wuhan, China.
16. J.D. Andrade (1985) X-ray Photoelectron Spectroscopy (XPS). In: J.D. Andrade (eds) Surface and Interfacial Aspects of Biomedical Polymers. Springer, Boston, MA.
17. V. V. Panić, A. B. Dekanski, T. R. Vidaković, V. B. Mišković-Stanković., *J. Solid State Electrochem.*, 9 (2005) 43.
18. J. Iniesta, P. A. Michaud, M. Panizza, Ch. Comninellis, *Electrochim. Acta*, 46 (2001) 3573.
19. M. Panizza, P. A. Michaud, Ch. Comninellis, *J. Electroanal. Chem.*, 507 (2001) 206.
20. S. Yang, H. Song, X. Chen, *Electrochem. Commun.*, 8 (2006) 137.
21. S. Zhang, P. Shi, *Electrochim. Acta*, 49 (2004) 1475.
22. C. Wan, Y. Nuli, J. Zhuang, Z. Jiang., *Mater. Letters*, 56 (2002) 357.
23. L.Z. Wang, Y. Zhao, S. Yang, B. Wu, P. Li, Y. Zhao, *Int. J. Electrochem. Sci.*, 11 (2016) 2401.
24. Y. Sun, P. Li, H. Zheng, C. Zhao, X. Xiao, Y. Xu, W. Sun, H. Wu, M. Ren, *Chem. Eng. J.*, 308 (2017) 1233.
25. W. Kong, B. Wang, H. Ma, L. Gu, *J. Hazard. Mater.*, 137 (2006) 1532.

© 2018 The Authors. Published by ESG ([www.electrochemsci.org](http://www.electrochemsci.org)). This article is an open access article distributed under the terms and conditions of the Creative Commons Attribution license (<http://creativecommons.org/licenses/by/4.0/>).